Mitochondrial H_2O_2 generation using a tunable chemogenetic tool to perturb redox homeostasis in human cells and induce cell death

Kassi T. Stein, Sun Jin Moon, Hadley D. Sikes[1]

Department of Chemical Engineering; Massachusetts Institute of Technology; Cambridge, MA, 02139, USA.

Abstract:

Among reactive oxygen species (ROS), H_2O_2 alone acts as a signaling molecule that promotes diverse phenotypes depending on the intracellular concentration. Mitochondria have been suggested as both sources and sinks of cellular H_2O_2, and mitochondrial dysfunction has been implicated in diseases such as cancer. A genetically-encoded H_2O_2 generator, D-amino acid oxidase (DAAO), was targeted to the mitochondria of human cells, and its utility in investigating cellular response to a range of H_2O_2 doses over time was assessed. Organelle-specific peroxiredoxin dimerization and protein S-glutathionylation were measured as indicators of increased H_2O_2 flux due to the activity of DAAO. Cell death was observed in a concentration- and time-dependent manner, and protein oxidation shifted in localization as the dose increased. This work presents the first systematic study of H_2O_2-specific perturbation of mitochondria in human cells, and it reveals a marked sensitivity of this organelle to increases in H_2O_2 in comparison with prior studies that targeted the cytosol.

Keywords: hydrogen peroxide; redox regulation; mitochondria; chemogenetic tools; peroxiredoxin

Hydrogen peroxide (H_2O_2) is a member of a family of molecules known as reactive oxygen species (ROS) and has been demonstrated to induce proliferation, differentiation, and cell death [1,2]. Among ROS, H_2O_2 is known to behave as a classical signaling molecule, undergoing specific

[1] To whom correspondence should be addressed (sikes@mit.edu)

reactions with cysteine residues to cause various downstream effects [3–5]. It has been observed that the intracellular level of H_2O_2 determines phenotypic outcome, so controlled modulation of H_2O_2 concentration is desirable in order to probe cellular response [4]. Previous studies have investigated cytoplasmic generation of H_2O_2 and found either no toxic effects[6] or only partial toxicity with surprisingly large and lengthy perturbations[7].

It is thought that subcellular localization of H_2O_2 generation, in addition to concentration, determines downstream effects[1,4]. The need for mechanistic studies exploring the effects of targeted, intracellular H_2O_2 generation has already been identified, as the network of antioxidant reactions confine H_2O_2 to a small area near its generation site [8–11]. This limitation imposed by the interplay of reaction and diffusion rates within the cell highlights the difference between extracellular bolus addition and intracellular peroxide generation [11,12]. Mitochondria are a compelling organelle for study because they have been suggested as both sources and sinks of intracellular ROS, as well as a hypothesized site for redox signaling [5,13,14]. Mitochondria generate superoxide ($O_2^{\bullet-}$) at various points in the electron transport chain (ETC) as well as in the Kreb's cycle, after which it is quickly converted to H_2O_2 by manganese superoxide dismutase (MnSOD) [5]. The H_2O_2 levels are managed by the mitochondrial antioxidant network, which is dominated by the 2-cysteine peroxidase Peroxiredoxin 3 (Prx-3) [5,15].

Notably, mitochondrial H_2O_2 has been implicated in the onset of apoptosis as well as several diseases, such as cancer and diabetes; as such, some therapeutics have targeted mitochondria and mitochondrial ROS [13,16–18]. However, a dose-response relationship between mitochondrial H_2O_2 and cell phenotype, as well as the kinetics involved in this interaction, have not been well established. Synthetic biology tools provide access to this information, enabling elucidation of the strength and activities of compartment-specific networks of antioxidant

reactions. In our previous work, we used tunable tools in the cytosol of human epithelial cells to establish the concentration- and time-dependence of H_2O_2-induced cell death [7]. We observed only partial toxicity (<50%) as a result of these cytosolic H_2O_2 perturbations. Here, we extend this approach to mitochondria, enabling a comparison of cellular responses to compartment-specific

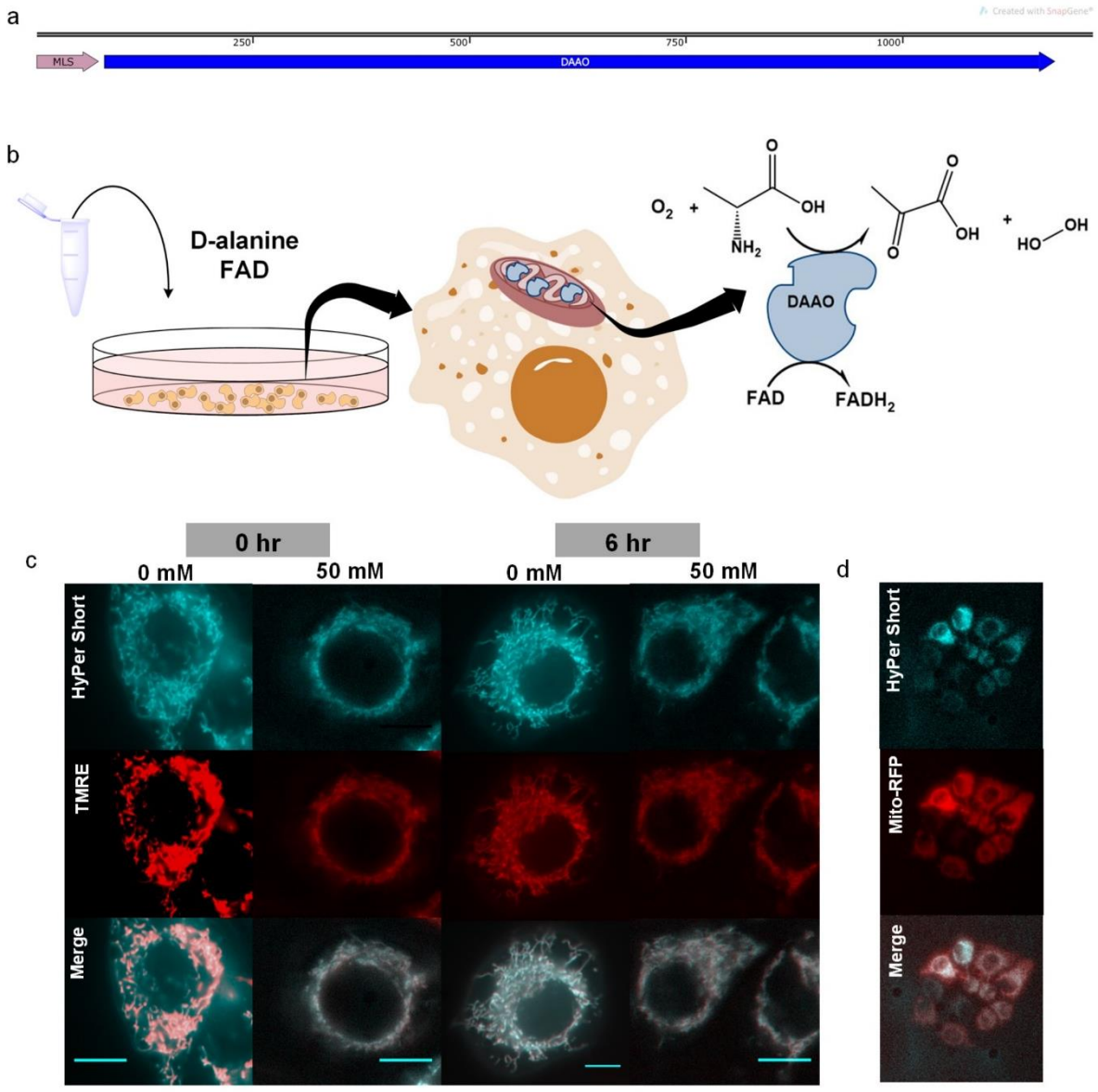

Figure 1: Schematic overview of synthetic construct and experimental mechanism. a) A mitochondrial localization sequence (MLS) on the N-terminus of the DAAO protein codes for the short peptide sequence necessary for protein import to the mitochondrial matrix. b) Cells expressing the synthetic DAAO-mito were exogenously given D-alanine and FAD to induce mitochondrial H_2O_2 generation in a dose-response fashion. DAAO performs oxidative deamination on D-alanine to produce pyruvate and H_2O_2 using FAD as a cofactor. c) Control cells not expressing DAAO-mito stimulated with 50 mM D-ala for 6.5 hours did not show signs of mitochondrial stress or toxicity. Scale bars represent 50 µm. Full microscopy images are shown in SI Figure S1. d) HeLa cells co-expressing DAAO-mito and HyPer-mito imaged with mito-RFP to verify mitochondrial localization of the biosensor HyPer.

perturbations.

We have implemented a tunable chemogenetic tool, a D-amino acid oxidase construct targeted to the mitochondrial matrix (DAAO-mito)[19] (Figure 1a), to systematically study the effects of elevated mitochondrial H_2O_2. Thus far, this tool has not been used in the mitochondria, so it is not yet understood how these perturbations might affect cells' downstream phenotypes. DAAO reacts with D-amino acids and oxygen to generate imino acids and H_2O_2 using flavin adenine dinucleotide (FAD) as a cofactor (Figure 1b). Here, we have used D-alanine (D-ala) to control the onset and amount of H_2O_2 produced. DAAO's reaction with D-ala is characterized by a Michaelis-Menten constant, K_m, in the mM concentration regime [20]. We stimulated cells with a range of H_2O_2 doses by supplying D-ala at concentrations ranging from 0 – 50 mM over periods of up to 6.5 hours. D-ala alone is not toxic to HeLa cells even at the highest concentration and time combination used (Figure 1c) so it is a viable substrate for these experiments. To validate the function of the tool in the mitochondria, cells were analyzed as a function of time for post-translational protein modifications that provide evidence of H_2O_2 generation. After dose-response trends were observed in two different kinds of molecular measurements, changes in mitochondrial morphology and membrane potentials, as well as phenotypic responses of cells to a range of perturbations were assessed. In order to monitor the morphological changes that took place as cells were perturbed with H_2O_2, the H_2O_2 biosensor HyPer was targeted to the mitochondria of HeLa cells, as presented in Figure 1d [21]. In contrast with destructive analysis techniques such as immunoblotting and immunocytochemistry, HyPer allows live-cell imaging; a commercially-available RFP targeted to the mitochondria was used to verify mitochondrial localization of HyPer-mito (Figure 1d). Considering these new results in the context of previous findings, increased H_2O_2 fluxes in the mitochondria are considerably more toxic than increased H_2O_2 fluxes in the

cytosol, and a mitochondrial permeability transition (MPT) rather than mitochondrial fragmentation accompanies this toxicity.

To assess function of DAAO in the mitochondria, the Peroxiredoxin (Prx) family of proteins was probed using redox Western blotting techniques to detect direct molecular evidence of changes in H_2O_2 (Figure 2). Increased fluxes of H_2O_2 in different organelles is detectable based on the oxidation status of different Prx isoforms [15,22]. In the cytoplasm, Prx-2 is expected to be the dominant antioxidant in the network involved in clearing physiologically relevant concentrations of H_2O_2 [9,11]. Similarly, in the mitochondria, Prx-3 is expected to dominate, with an abundance of 60 μM and a second-order rate constant of $2x10^7$ $M^{-1}s^{-1}$ [5,15]. Catalase, the most familiar scavenger of H_2O_2, is generally not found in mitochondria, or is found at concentrations nearly four orders of magnitude lower than Prx-3 in specialized tissues, so it is not expected to contribute appreciably to the mitochondrial antioxidant network [5,15]. Similarly, Glutathione peroxidase 1 (Gpx 1) is present at an order of magnitude lower concentration than Prx-3, so despite the fact that the second-order rate constant of Gpx 1 is similarly high at $6x10^7$ $M^{-1}s^{-1}$, it is expected to make at most a minor contribution to the mitochondrial antioxidant network [15].

Redox Western blots were performed on cell lysates to determine the relative changes in

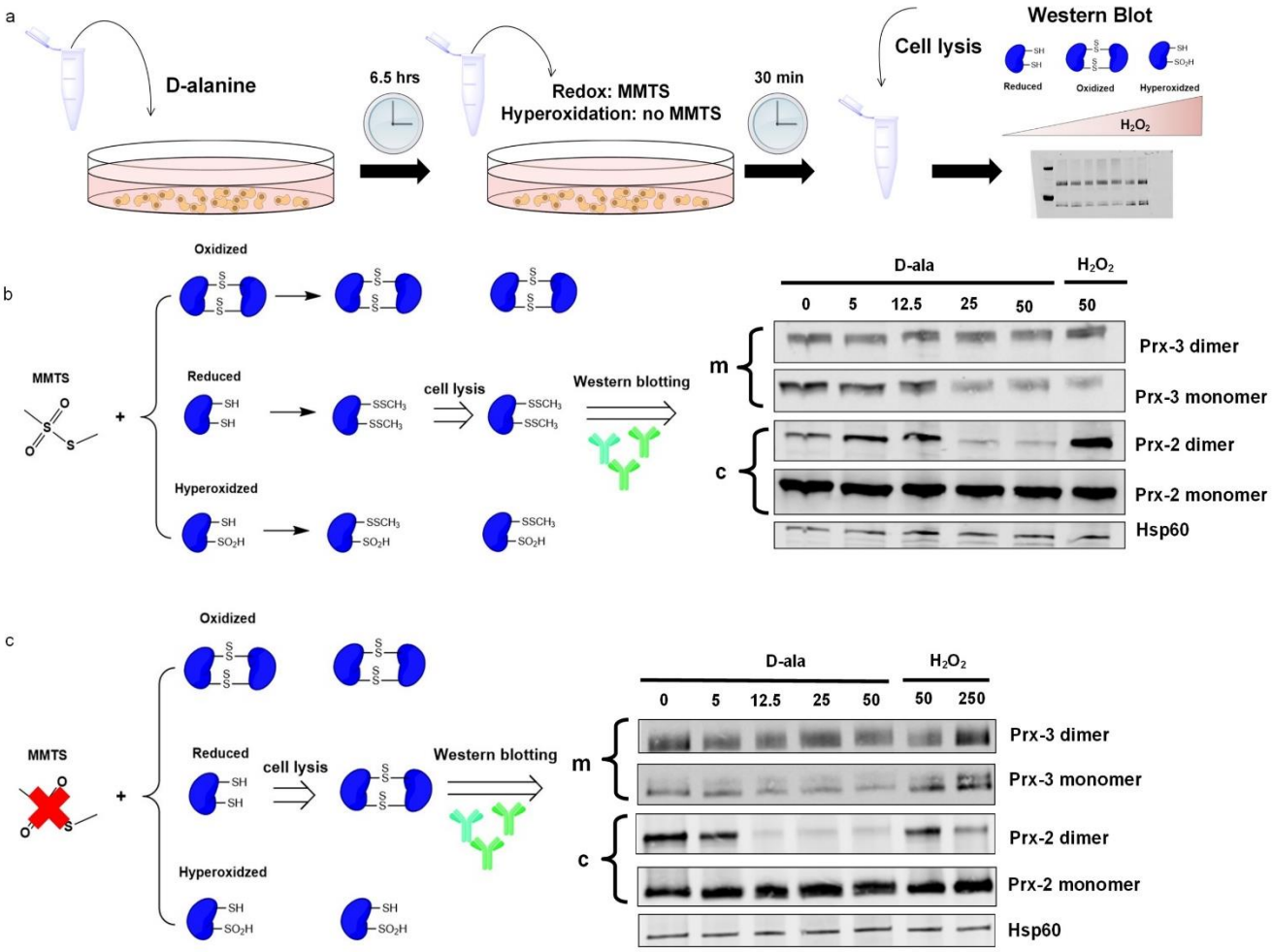

Figure 2: Redox Western Blots Demonstrate Increasing Mitochondrial and Cytoplasmic H_2O_2 upon Stimulation of DAAO-mito Cells with D-ala. a) HeLa cells co-expressing HyPer-mito and DAAO-mito were stimulated with the indicated concentration of D-ala (mM) for 6.5 hours or given the indicated bolus of H_2O_2 (μM) as a positive control. Then cells were either blocked with the alkylating agent methyl methanethiosulfonate (MMTS), which reacts with free thiols (Redox western blot, b), prior to cell lysis or lysed without alkylating agents (Hyperoxidation western blot, c). b) Redox blots for Prx-3 and Prx-2. Dimerized species indicate oxidation, as indicated in the schematic. The disappearance of the Prx-2 dimer at higher concentrations of D-ala suggests hyperoxidation, implying high concentrations of H_2O_2 in the cytosol. c) Hyperoxidation blots, where disappearance of dimer species indicates hyperoxidation, as indicated in the schematic. Suspected hyperoxidation from b) is confirmed by the disappearance of the Prx-2 dimers. Corresponding densitometry plots, tabulates densitometry data, and full blot images for both b) and c) are presented in SI Figures S2-S7 and Table S1.

reduced and oxidized Prx-2 and Prx-3 across the different treatments, as schematically depicted in Figure 2a. Methyl methanethiosulfonate (MMTS) was reacted with cultures prior to lysis to convert sulfhydryl groups to -SS-CH_3 groups (Figure 2b), so increases in the dimer Prx species from the 0 mM D-ala are indicators of intracellular H_2O_2 fluxes rather than lysis-induced oxidation artifacts. Analogously, the reduced status of monomers is preserved. Analysis of mitochondrial

Prx-3 in Figure 2b demonstrates that, as more peroxide was generated, the amount of monomer decreased, with a resulting increase in the amount of dimer. This finding is consistent with what one would expect from the local action of H_2O_2. In the cytoplasm, at low doses of H_2O_2, there was an increase from control in the dimer band of Prx-2. Interestingly, however, the dimer bands disappeared at higher levels of H_2O_2, implying either suddenly low levels of H_2O_2 or hyperoxidation, as Prx-2 cannot dimerize when its thiol has been hyperoxidized to a sulfinic or sulfonic acid [3,23]. To confirm whether this was indeed hyperoxidation and not simply reduced Prx-2, a Western blot was performed without any MMTS thiol-blocking steps prior to cell lysis; disappearance of the dimer indicates hyperoxidation [23]. This methodology following the protocol established by Cox *et al.* was preferred over blotting with antibodies specific to the sulfinic/sulfonic forms of Prx because existing antibodies are not specific to particular Prx isoforms, ergo all compartment-specific information is lost [23]. Figure 2c depicts the results of the hyperoxidation blot, which confirm that at low levels of H_2O_2 generation in the mitochondria, Prx-2 did not differ from control, but at higher levels of H_2O_2, Prx-2 became hyperoxidized in the cytoplasm. These results suggest that large amounts of H_2O_2 were present in the cytoplasm above some threshold of mitochondrial H_2O_2 generation, as more than 150 nM of cytosolic H_2O_2 (~100 µM external bolus) would be necessary to induce this reaction [24]. In summary, redox (+MMTS) and hyperoxidation (-MMTS) Western blots of Prx-3 (mitochondrial) and Prx-2 (cytosolic) oxidation states validated the function of DAAO-mito in elevating H_2O_2 flux in the mitochondria, and increases in H_2O_2 flux appeared to correlate with the concentration of D-ala, substrate of DAAO.

To further validate the function of the tool and test for dose-dependent molecular modifications of proteins, we examined protein S-glutathionylation (Pr-SSG). This post-

translational modification results when a cysteine residue of a protein is oxidized by H_2O_2 to form a sulfenic acid. The sulfenic acid form of the protein then reacts with glutathione to form a disulfide linkage between the protein and glutathione (Pr-SSG). Protein S-glutathionylation has been hypothesized to be important in the redox regulation of mitochondria. The primary proposed role for Pr-SSG is to protect proteins from further oxidation; the mixed disulfide bond with glutathione is readily reduced by glutaredoxin (Grx), whereas a sulfinic or sulfonic acid is not so easily reversed. It has also been proposed that Pr-SSG regulates protein function as a post-translational modification, especially in the mitochondria [25]. Cells were therefore probed for Pr-SSG conjugates using immunofluorescence. Figure 3 demonstrates that, as H_2O_2 dose increases due to stimulation of DAAO-mito with D-ala, the abundance of Pr-SSG increases as well. In addition, the pattern of Pr-SSG shifts from localized at low H_2O_2 concentrations to ubiquitous at high H_2O_2 concentrations; the single-cell images in Figure 3b better illustrate this change. The distribution of feature sizes is shown in Figure 3d, and demonstrates a marked shift from small features at low D-ala concentrations, to distributions that span several orders of magnitude at 25 mM, shown by the peak flattening as D-ala concentration increases. This finding suggests that at low levels, the effects of H_2O_2 signaling are localized, but at high levels, those effects are no longer confined to subcellular regions. Additionally, the observed staining pattern coupled with the changes in Prx oxidation suggest some kind of threshold in cellular response between 12.5 and 25 mM D-ala.

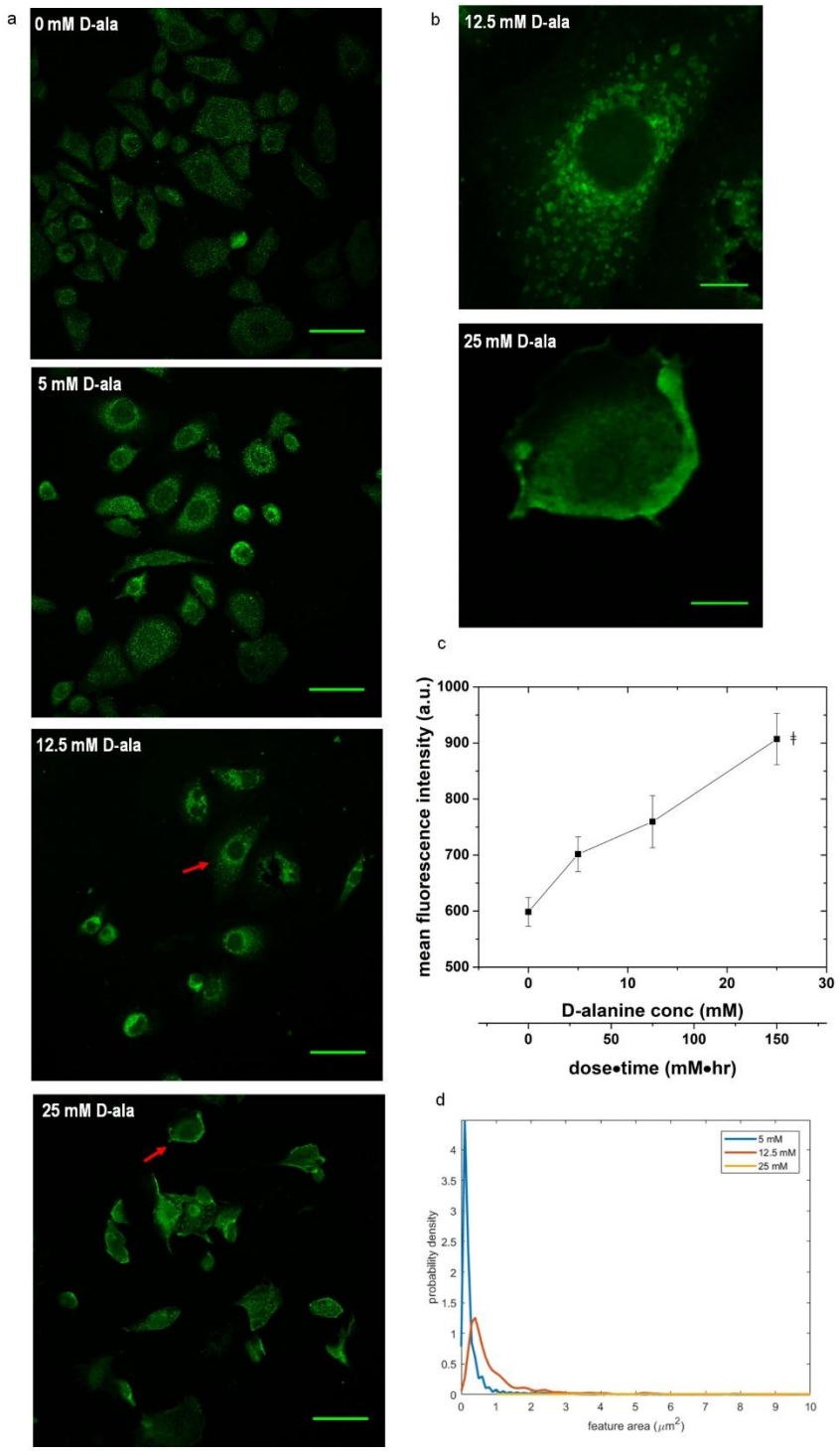

Figure 3: Pr-SSG Abundance and Localization Depends on H_2O_2 Dose. a) HeLa cells co-expressing HyPer-mito and DAAO-mito stimulated with the indicated concentration of D-ala for 6 hours, labeled with an antibody specific for protein-GSH conjugates. Signal at 0 mM D-ala indicates baseline Pr-SSG. Scale bars represent 50 μm. b) Close-up of cells indicated by red arrows in a. Scale bar represents 10 μm. c) Mean fluorescence intensity vs. D-ala concentration of the cells stained for Pr-SSG. Points represent mean ± SEM of the cells across four fields of view. ǂ denotes $P<0.005$ by ANOVA. d) Probability distribution of feature sizes identified by Pr-SSG staining, given by the area in μm^2.

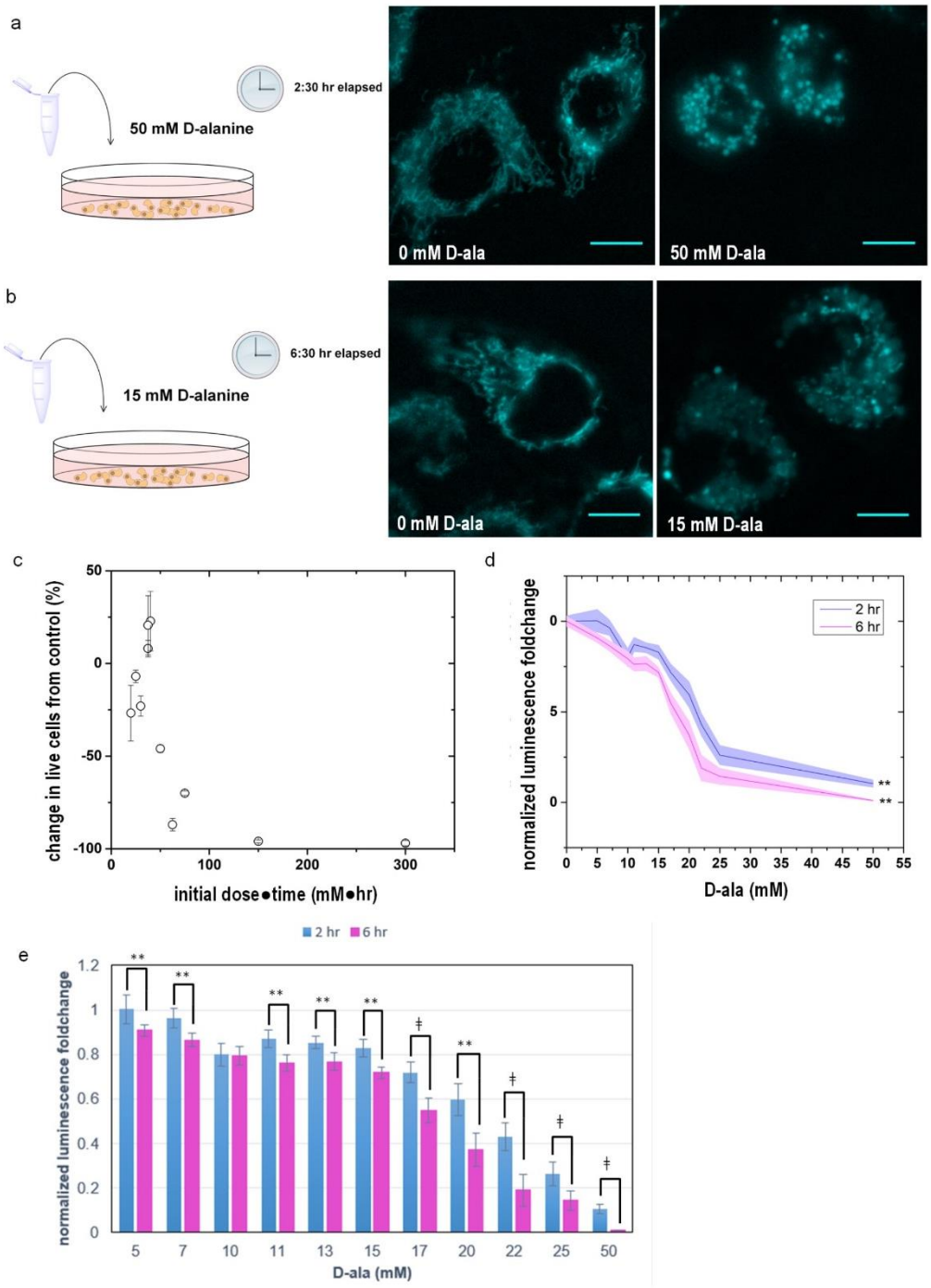

*Figure 4: Localizing a H_2O_2 Perturbation to the Mitochondria Causes Morphological Changes and Cell Death. a) HeLa cells co-expressing HyPer-mito and DAAO-mito stimulated with 50 mM D-ala for 2.5 hours. b) HeLa cells co-expressing HyPer-mito and DAAO-mito stimulated with 15 mM D-ala for 6.5 hours. Additional microscopy images for a) and b) can be found in SI Figure S8. c) Decrease in live cells as measured by Trypan blue exclusion compared to control (0 mM D-ala) vs. the initial dose of D-ala multiplied by treatment time (mM·hr). Points represent mean ± SEM. d) Normalized luminescence foldchange, as measured by CellTiter Glo, for cells treated with D-ala for 2 hours (blue) and 6 hours (magenta). Lower luminescence corresponds to lower cell viability. Lines represent the average of 16 cultures, and shaded regions represent SEM. ** denotes P<0.05 for ANOVA. e) Data from d represented as a bar chart to more clearly show the differences between 2 and 6 hours. ** denotes P<0.05, ǂ denotes P<0.001 for one-tailed t-test.*

Once specific, molecular evidence of H_2O_2-mediated reactions had been established, it was next of interest to investigate downstream phenotypic responses, including morphological changes to mitochondria as well as cell fate decisions. Unperturbed cells displayed a string-like mitochondrial morphology, consistent with published descriptions of healthy mitochondria (Figure 4b-c, 0 mM D-ala) [26]. Cells co-expressing DAAO-mito and HyPer-mito were monitored at various intervals over the generation periods, up to 7 hours, with D-ala concentrations of 0 – 50 mM to note any changes. Figure 4 depicts representative results of these experiments, with Figure 4a showing a short, high intensity D-ala perturbation and Figure 4b showing a longer, lower intensity D-ala perturbation. At shorter generation times, the highest concentrations of H_2O_2 had induced drastic morphological changes (Figure 4a) and cell detachment. Mitochondria became swollen and punctate, consistent with qualitative signs of mitochondrial stress. Lower concentrations of H_2O_2 did not induce these morphological changes until longer generation times (Figure 4b). This was indicative of a temporal component to H_2O_2-induced toxicity in the mitochondria, consistent with previous findings in the cytoplasm [7]. Change in live cells is plotted as a function of D-ala dose·time [mM·hr] in Figure 4c for all perturbations, demonstrating a trend of increasing toxicity with increasing dose·time combinations, with a 98% decrease in cell survival observed with the highest dose·time combination of 300 mM·hr. This trend is echoed in the cell viability data obtained by CellTiter Glo assay, depicted in Figure 4d-e. Holding dosing time constant, cell viability decreases as a function of D-ala concentration, plotted in Figure 4d. On the other hand, holding concentrations constant, cell viability also decreases as a function of dosing time, depicted in the bar chart in Figure 4e. Though we calculated HyPer ratios during these experiments and observed an increasing trend with increasing D-ala concentration, cell-to-cell heterogeneity made the probe more useful for observing morphological changes than for exact quantification of H_2O_2 in these

long-term experiments where monitoring individual cells for the duration of the experiment was not practical (SI Figures S9 – S10).

Punctate mitochondrial morphology and mitochondrial swelling is typical of cell stress [27]**.** A mitochondrial depolarization assay was performed in order to attribute this morphological change to mitochondrial fragmentation or mitochondrial permeability transition (MPT); an increase in mitochondrial polarization would indicate the former, while a decrease implies the latter [26,28]. As demonstrated in Figure 5, using the cationic lipophilic dye tetramethylrhodamine ethyl ester (TMRE), mitochondria were initially polarized, indicated by the bright TMRE fluorescence. As H_2O_2 was generated, polarization was lost, as indicated by the loss in TMRE fluorescence signal. The dark panel at 50 mM D-ala (325 mM·hr) in Figure 5a indicates the complete depolarization at the highest dose of H_2O_2 assayed, demonstrating that mitochondria became completely depolarized over the investigated dose range. The plot in Figure 5b marks the trend of decreasing TMRE fluorescence as the mitochondria were exposed to increasing doses of H_2O_2. These data are consistent with changes associated with the MPT.

Uncovering the signaling reactions underlying the mechanism of cell death initiated by mitochondrial H_2O_2 generation is an intriguing line of study prompted by these results.

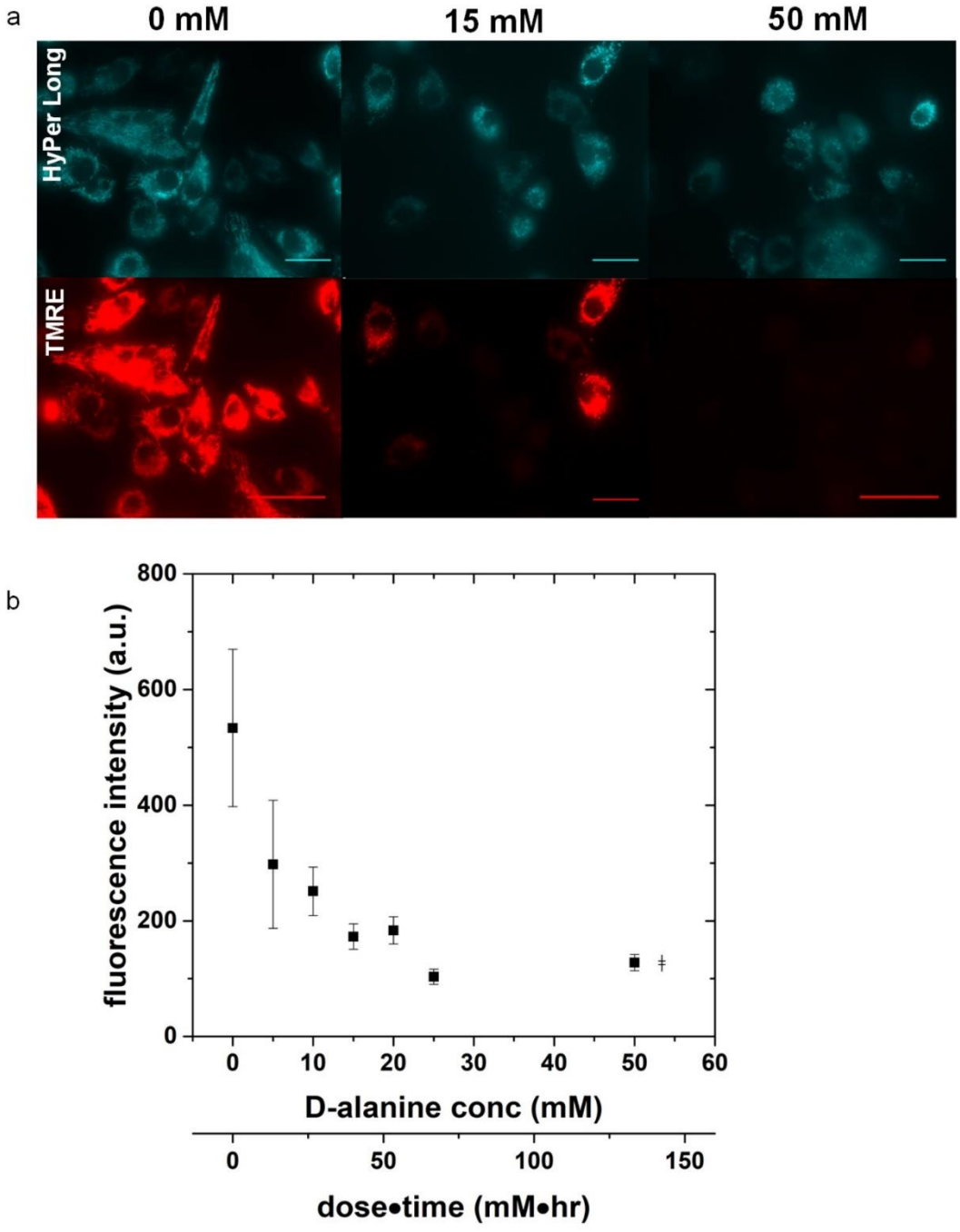

Figure 5: Mitochondrial Depolarization Assay Consistent with MPT. a) HeLa cells co-expressing HyPer-mito and DAAO-mito stimulated with the indicated concentration of D-ala for 6.5 hr. More concentrations shown in SI Figure S11. HyPer Long signal shown on the top row and TMRE signal shown on the bottom row. Scale bars represent 50 μm. b) Trend in average TMRE signal across D-ala doses after 2.75 hr of stimulation. Points represent mean ± SEM of at least four fields of view. ǂ indicates P<0.005 by ANOVA.

Understanding how the cell death signal is being transmitted, and which proteins are involved, will enable better manipulation of the cellular environment for therapeutic purposes. Several proteins in the mitochondria are hypothesized to be redox-sensitive and targets for signaling via H_2O_2, including the adenine nucleotide translocase (ANT), which plays a role in the mitochondrial permeability transition pore (MPTP) [29]. In addition, Prx-3 itself is thought to play a role in signal transduction [5,15,30]. The transcription factor signal transducer and activator of transcription 3 (STAT3) has also been described as a redox-responsive signaling molecule, responding to changes in H_2O_2 levels throughout the cell and propagating the signal downstream [31,32]. STAT3 is now thought to play several important roles in the mitochondria, including regulation of the MPTP [31]. While there are missing links in how the cell converts the input of H_2O_2 into a cell death signal, this work has demonstrated the ability to make controlled perturbations in order to study these pathways mechanistically. Investigating spatiotemporal aspects of H_2O_2 reactions and signaling will provide important supplementary information to existing bolus-addition-based experiments.

Finally, one of the most notable aspects of this work is the dramatic increase in cell death with H_2O_2 generation in the mitochondria compared to control. Previous work in the cytoplasm demonstrated at most an approximately 45% increase in toxicity compared to control, much lower than the 98% decrease in survival observed with mitochondrial localization, even with shorter generation times [7]. It is thought that redox-based therapeutics work by raising the levels of intracellular oxidants, though the mechanisms are only beginning to be understood. This work suggests that redox-based chemotherapeutics may be more deleterious to cells if targeted to the mitochondria, as previously hypothesized [33]. Efforts exist to both target existing redox-active compounds to the mitochondria and also understand the mechanisms of compounds that seem to act via the mitochondria [34,35]. Making controlled perturbations with a peroxide generator has been

useful in elucidating drug mechanisms in the cytoplasm, and could be a key tool in understanding chemotherapeutics in the mitochondria [36].

Methods:

Cell Culture:

HeLa cells were a generous gift from Dane Wittrup, and were maintained in Dulbecco's modified Eagle's medium (DMEM; Lonza) supplemented with 10% fetal bovine serum (FBS; ATCC) at 37 ºC in a humidified atmosphere of 5% CO_2. Cells were passaged every three to six days, depending on growth rate. Stable cell lines created by lentivirus transfection using a synthetic construct were maintained in medium containing 6 μg/mL puromycin (Sigma) to apply selective pressure. Detailed transfection information can be found in Supporting Information.

Mitochondrial Generation of H_2O_2 Using D-amino Acid Oxidase:

HeLa cells co-transfected with HyPer-mito and DAAO-mito were seeded at $3.5x10^5$ cells/well in 35 mm dishes or 6-well plates, $1.75x10^5$ cells/well in 12-well plates coated with poly-L-lysine (Sigma), or $2x10^4$ cells/well in 96-well plates 24 hours prior to the start of generation. For confocal imaging experiments, cells were grown on 12 mm round coverslips coated with poly-L-lysine (Fisher Scientific) seeded at $8.75x10^4$ cells/well. Cells were washed once with 1x PBS then exposed to 5 μM FAD (Sigma) and concentrations of D-alanine (Sigma) from 0 – 50 mM in Roswell Park Memorial Institute 1640 medium (RPMI; Invitrogen) without phenol red. At least 25 cells per time point per condition were imaged.

Redox Western Blotting*:*

The protocols for redox western blotting were adapted from [23]. Prior to lysing, cells grown in 6-well plates were washed with 1x PBS then incubated on ice with 2 mL 100 mM methyl

methanethiosulfonate (MMTS; Sigma) for 30 min to block thiols. Cells were lysed with 100 µL lysis buffer (0.5% Triton X-100, 1x HALT protease inhibitors (ThermoFisher), 1x PBS) then lysates were collected and centrifuged at 10,000 xg for 10 min. Supernatants were separated on a non-reducing SDS-PAGE 12% polyacrylamide gel, then transferred to a PVDF membrane for immunoblotting. Blots were blocked with Odyssey blocking buffer (Licor) and incubated overnight at 4 °C with primary antibodies against Prx-2 (R&D Systems, AF3489), Prx-3 (Abcam, Clone# EPR8115), and Hsp60 (R&D Systems, Clone# 264233). Blots were incubated with IR-conjugated secondary antibodies (Licor) for 1 hr at room temperature. For the Western blots showing hyperoxidation, the same protocol was followed, excluding the blocking step with MMTS.

Protein S-glutathionylation Immunofluorescence*:*

After H_2O_2 generation experiments, cells were fixed in 4% paraformaldehyde for 30 min. Cells were permeabilized in 0.5% Triton X-100 (Sigma) in 1x PBS for 30 min and blocked in 2% bovine serum albumin (BSA; VWR), 0.5% Triton X-100 in 1x PBS for 30 min. Primary antibody staining with antibodies raised against protein-glutathione conjugates (Abcam, Clone# D8) was performed overnight at 4 °C at a 1:200 dilution. AlexaFluor-488 conjugated (Invitrogen) secondary antibody staining was performed for 45 min at room temperature at a 1:250 dilution. Feature sizes were quantified using a built-in toolbox in ImageJ. We note that we have verified the specificity of the Pr-SSG antibody used here by reducing the mixed disulfides induced by DAAO/D-ala H_2O_2 perturbations and observing the expected ablation of fluorescent signal upon immunofluorescent analysis [36].

Cell Viability after Exposure to H_2O_2 Produced by DAAO-mito:

For cell counts, at the end of H_2O_2 generation experiments, cells were trypisinized and counted by Trypan blue exclusion to obtain live cell counts. For CellTiter Glo, cells were grown in white 96-well plates. Assay was performed according to manufacturer's instructions.

Mitochondrial Depolarization Assay*:*

Prior to treatment of cells with D-alanine, cells were incubated with 200 nM tetramethylrhodamine, ethyl ester (TMRE; ThermoFisher) for 45 min spiked directly into the culture medium. 20 µM Carbonyl cyanide-p-trifluoromethoxyphenylhydrazone (FCCP; Sigma) was used as a positive control for mitochondrial depolarization, and was added 10 min prior to TMRE addition. After dye incubation, cells were washed once with Dulbecco's phosphate buffered saline (DPBS) with calcium and magnesium (ThermoFisher), and then culture medium was replaced with RPMI for H_2O_2 generation and imaging. At least four images per condition per time were taken. TMRE-stained images were quantified using ImageJ by measuring the average fluorescence of the entire field of view.

Fluorescence Microscopy:

The ratiometric HyPer-mito signal was captured using an inverted IX81 widefield fluorescence microscope (Olympus) with a 60x/1.42 NA oil-immersion objective lens and Prior Lumen2000 lamp. For the HyPer Short channel, a Chroma 415/30 nm excitation filter was used, and for the HyPer Long channel, a Semrock 488/6 nm excitation filter was used. Emission was collected on a Semrock 525/40 nm filter for both channels. A 250 ms exposure time and 10% lamp intensity was used to generate fluorescent images. Mitochondrial localization was verified using CellLight Mitochondria-RFP, BacMam 2.0 (ThermoFisher) following manufacturer's instructions. TMRE and CellLight Mitochondria-RFP were visualized using a Texas Red filter set from Semrock, 562/40 nm excitation and 624/40 nm emission, and AlexaFluor-488 conjugated secondary

antibodies were visualized using a GFP filter set from Semrock, 472/30 nm excitation and 520/35 nm emission. Confocal images were obtained using a FV1000MPE confocal microscope (Olympus) and a 40x/1.25 NA oil-immersion objective lens. Images were exported to ImageJ or MATLAB for post-processing.

Quantification and Statistical Analysis:

At least four fields of view per time point per condition were captured for all imaging experiments, encompassing a minimum of 20-70 cells total. The number of cells observed per condition was inversely proportional to the toxicity of the perturbation, as this factor limited the number of cells available for analysis. A minimum of two biological replicates and three technical replicates per experiment were performed (a minimum of four technical replicates for imaging experiments). Analysis of variance (ANOVA) or Welch's ANOVA testing of trends was performed where appropriate using the Excel Real Statistics add-in. The null hypothesis in this case is that all sample means for all concentrations of D-ala assayed are equal. One-tailed Student's t tests were calculated using the built-in Excel statistics toolbox.

Supporting Information

The following Supporting Information is available free of charge on the ACS Publications website at DOI:

uncropped and additional microscopy images, uncropped western blots, quantification of bands in western blots, quantification of HyPer ratios, procedures for creation of stable cell lines, sequence of DAAO-mito construct

Author Contributions:

Conceptualization, K.T.S. and H.D.S.; Methodology, K.T.S.; Investigation, K.T.S. and S.J.M.; Formal Analysis, K.T.S.; Writing – Original Draft, K.T.S. and H.D.S.; Writing – Review &

Editing, K.T.S. and H.D.S.; Supervision, H.D.S.

Acknowledgements:

A Wade Fund Award from MIT's Research Support Committee funded this work. K.S. acknowledges the NSF Graduate Research Fellowship Program. The PLJM1-EGFP plasmid was a gift from David Sabatini (Addgene plasmid #19319). The psPAX2 and pMD2.G plasmids were gifts from Didier Trono (Addgene plasmids #12260 and #12259). The DAAO-mito plasmid was a gift from Rajiv Ratan at Weill Medical College of Cornell University. We thank Justin Swaney in the Chung Lab at MIT for his help obtaining the confocal images. We thank Jaime Cheah and Christian Soule of the Koch Institute High-Throughput Screening Core for their help obtaining the CellTiter Glo data, as well as many helpful discussions.

References:

(1) Sies, H. (2017) Hydrogen peroxide as a central redox signaling molecule in physiological oxidative stress: Oxidative eustress. *Redox Biol. 11*, 613–619.
(2) D'Autréaux, B., and Toledano, M. B. (2007) ROS as signalling molecules: mechanisms that generate specificity in ROS homeostasis. *Nat. Rev. Mol. Cell Biol. 8*, 813–824.
(3) Lennicke, C., Rahn, J., Lichtenfels, R., Wessjohann, L. A., and Seliger, B. (2015) Hydrogen peroxide – production, fate and role in redox signaling of tumor cells. *Cell Commun. Signal. 13*, 39.
(4) Gough, D. R., and Cotter, T. G. (2011) Hydrogen peroxide: a Jekyll and Hyde signalling molecule. *Cell Death Dis. 2*, e213.
(5) Rhee, S. G., and Kil, I. S. (2016) Mitochondrial H2O2 signaling is controlled by the concerted action of peroxiredoxin III and sulfiredoxin: Linking mitochondrial function to circadian rhythm. *Free Radic. Biol. Med. 100*, 73–80.
(6) Matlashov, M. E., Belousov, V. V., and Grigori, E. (2014) How Much H2O2 Is Produced by Recombinant D-Amino Acid Oxidase in Mammalian Cells? *Antioxid. Redox Signal. 20*, 1039–44.
(7) Huang, B. K., Stein, K. T., and Sikes, H. D. (2016) Modulating and Measuring Intracellular H 2 O 2 Using Genetically Encoded Tools to Study Its Toxicity to Human Cells. *ACS Synth. Biol. 5*, 1389–1395.
(8) Liou, G.-Y., and Storz, P. (2010) Reactive oxygen species in cancer. *Free Radic. Res. 44*, 479–496.
(9) Lim, J. B., Huang, B. K., Deen, W. M., and Sikes, H. D. (2015) Analysis of the lifetime and spatial localization of hydrogen peroxide generated in the cytosol using a reduced kinetic model. *Free Radic. Biol. Med. 89*, 47–53.
(10) Lim, J. B., Langford, T. F., Huang, B. K., Deen, W. M., and Sikes, H. D. (2016) A reaction-

diffusion model of cytosolic hydrogen peroxide. *Free Radic. Biol. Med. 90*, 85–90.
(11) Winterbourn, C. C. (2008) Reconciling the chemistry and biology of reactive oxygen species. *Nat. Chem. Biol. 4*, 278–286.
(12) Sobotta, M. C., Barata, A. G., Schmidt, U., Mueller, S., Millonig, G., and Dick, T. P. (2013) Exposing cells to H2O2: A quantitative comparison between continuous low-dose and one-time high-dose treatments. *Free Radic. Biol. Med. 60*, 325–335.
(13) Kang, J., and Pervaiz, S. (2012) Mitochondria: Redox Metabolism and Dysfunction. *Biochem. Res. Int. 2012*, 1–14.
(14) Shadel, G. S., and Horvath, T. L. (2015) Mitochondrial ROS Signaling in Organismal Homeostasis. *Cell 163*, 560–569.
(15) Cox, A. G., Winterbourn, C. C., and Hampton, M. B. (2010) Mitochondrial peroxiredoxin involvement in antioxidant defence and redox signalling. *Biochem. J. 425*, 313–325.
(16) Cao, X., Zhao, S., Liu, D., Wang, Z., Niu, L., Hou, L., and Wang, C. (2011) ROS-Ca2+ is associated with mitochondria permeability transition pore involved in surfactin-induced MCF-7 cells apoptosis. *Chem. Biol. Interact. 190*, 16–27.
(17) Milane, L., Trivedi, M., Singh, A., Talekar, M., and Amiji, M. (2015) Mitochondrial Biology, Targets, and Drug Delivery. *J. Control. Release 207*, 40–58.
(18) Sullivan, L. B., and Chandel, N. S. (2014) Mitochondrial reactive oxygen species and cancer. *Cancer Metab. 2*, 17.
(19) Alim, I., Haskew-Layton, R. E., Aleyasin, H., Guo, H., and Ratan, R. R. (2014) Spatial, Temporal, and Quantitative manipulation of Intracellular Hydrogen Peroxide in Cultured Cells. *Methods Enzymol. 547*, 251–273.
(20) Pollegioni, L., Langkau, B., Tischer, W., Ghisla, S., and Pilone, M. S. (1993) Kinetic mechanism of D-amino acid oxidases from Rhodotorula gracilis and Trigonopsis variabilis. *J. Biol. Chem. 268*, 13850–13857.
(21) Belousov, V. V, Fradkov, A. F., Lukyanov, K. A., Staroverov, D. B., Shakhbazov, K. S., Terskikh, A. V, and Lukyanov, S. (2006) Genetically encoded fluorescent indicator for intracellular hydrogen peroxide. *Nat. Methods 3*, 281–286.
(22) Pastor-Flores, D., Becker, K., and Dick, T. P. (2017) Monitoring yeast mitochondria with peroxiredoxin-based redox probes: the influence of oxygen and glucose availability. *Interface Focus 7*, 20160143.
(23) Cox, A. G., Winterbourn, C. C., and Hampton, M. B. (2010) Measuring the Redox State of Cellular Peroxiredoxins by Immunoblotting, in *Methods in enzymology* 1st ed., pp 51–66. Elsevier Inc.
(24) Huang, B. K., and Sikes, H. D. (2014) Quantifying intracellular hydrogen peroxide perturbations in terms of concentration. *Redox Biol. 2*, 955–962.
(25) Mailloux, R. J., and Treberg, J. R. (2016) Protein S-glutathionlyation links energy metabolism to redox signaling in mitochondria. *Redox Biol. 8*, 110–118.
(26) Liesa, M., and Shirihai, O. S. (2013) Mitochondrial dynamics in the regulation of nutrient utilization and energy expenditure. *Cell Metab. 17*, 491–506.
(27) Dvorakova, K., Waltmire, C. N., Payne, C. M., Tome, M. E., Briehl, M. M., and Dorr, R. T. (2001) Induction of mitochondrial changes in myeloma cells by imexon. *Blood 97*, 3544–3551.
(28) Zorov, D. B., Filburn, C. R., Klotz, L.-O., Zweier, J. L., and Sollott, S. J. (2000) Reactive Oxygen Species (ROS)-induced ROS Release: A New Phenomenon Accompanying Induction of the Mitochondrial Permeability Transition in Cardiac Myocytes. *J. Exp. Med. 192*, 1001–1014.
(29) Halestrap, A. P., and Brenner, C. (2003) The Adenine Nucleotide Translocase: A Central

Component of the Mitochondrial Permeability Transition Pore and Key Player in Cell Death. *Curr. Med. Chem. 10*, 1507–1525.
(30) Cox, A. G., Pullar, J. M., Hughes, G., Ledgerwood, E. C., and Hampton, M. B. (2008) Oxidation of mitochondrial peroxiredoxin 3 during the initiation of receptor-mediated apoptosis. *Free Radic. Biol. Med. 44*, 1001–1009.
(31) Meier, J. A., Hyun, M., Cantwell, M., Raza, A., Mertens, C., Raje, V., Sisler, J., Tracy, E., Torres-Odio, S., Gispert, S., Shaw, P. E., Baumann, H., Bandyopadhyay, D., Takabe, K., and Larner, A. C. (2017) Stress-induced dynamic regulation of mitochondrial STAT3 and its association with cyclophilin D reduce mitochondrial ROS production. *Sci. Signal. 10*, eaag2588.
(32) Sobotta, M. C., Liou, W., Stöcker, S., Talwar, D., Oehler, M., Ruppert, T., Scharf, A. N. D., and Dick, T. P. (2014) Peroxiredoxin-2 and STAT3 form a redox relay for H2O2 signaling. *Nat. Chem. Biol. 11*, 64–70.
(33) Vyas, S., Zaganjor, E., and Haigis, M. C. (2016) Mitochondria and Cancer. *Cell 166*, 555–566.
(34) Galina, A. (2014) Mitochondria: 3-bromopyruvate vs. mitochondria? A small molecule that attacks tumors by targeting their bioenergetic diversity. *Int. J. Biochem. Cell Biol. 54*, 266–271.
(35) Smith, M. R., Vayalil, P. K., Zhou, F., Benavides, G. A., Beggs, R. R., Golzarian, H., Nijampatnam, B., Oliver, P. G., Smith, R. A. J., Murphy, M. P., Velu, S. E., and Landar, A. (2016) Mitochondrial thiol modification by a targeted electrophile inhibits metabolism in breast adenocarcinoma cells by inhibiting enzyme activity and protein levels. *Redox Biol. 8*, 136–148.
(36) Huang, B. K., Langford, T. F., and Sikes, H. D. (2016) Using Sensors and Generators of H2O2 to Elucidate the Toxicity Mechanism of Piperlongumine and Phenethyl Isothiocyanate. *Antioxid. Redox Signal. 24*, 924–938.

Supporting Information

Mitochondrial H_2O_2 generation using a tunable chemogenetic tool to perturb redox homeostasis in human cells and induce cell death

Kassi T. Stein, Sun Jin Moon, Hadley D. Sikes[1]

Department of Chemical Engineering; Massachusetts Institute of Technology; Cambridge, MA, 02139, USA.

[1] To whom correspondence should be addressed (sikes@mit.edu)

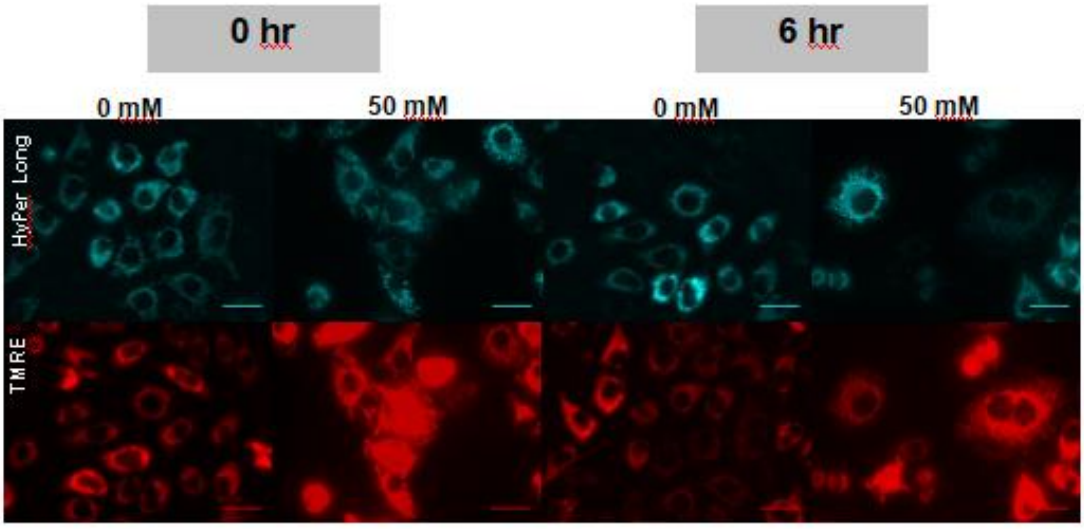

Figure S1: Full microscopy images for Figure 1d. Scale bars represent 50 µm.

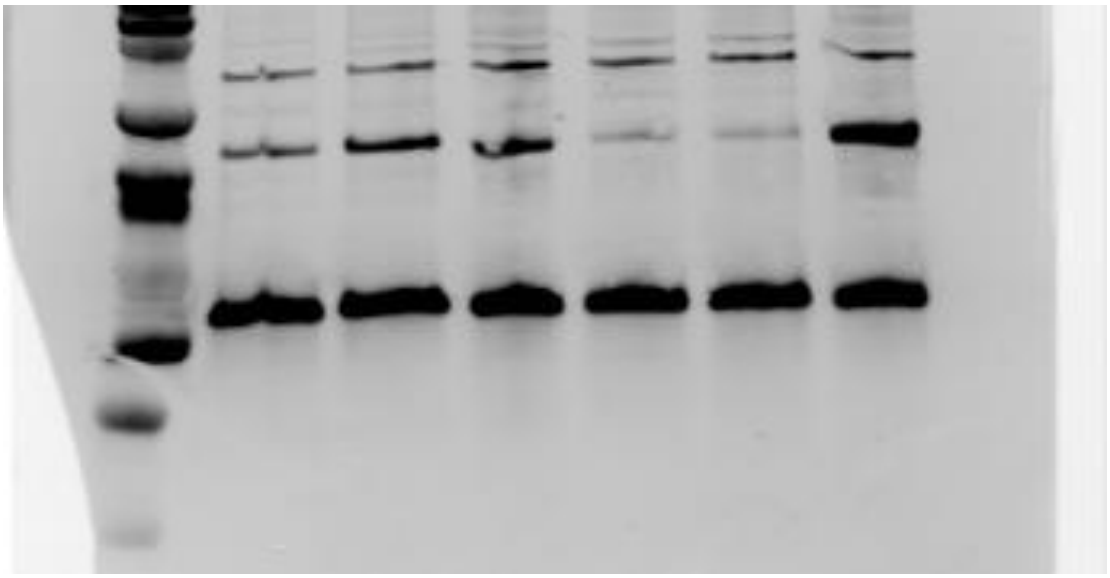

Figure S2: Full redox Western blot image from Figure 2, depicting bands for Hsp60 (top), Prx-2 dimer (middle), and Prx-2 monomer (bottom).

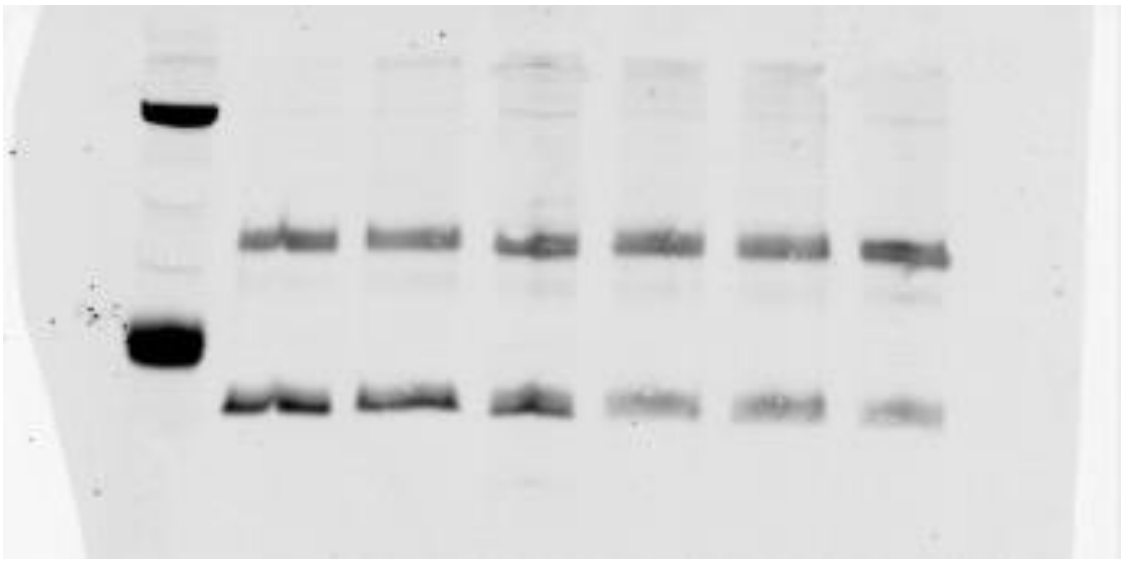

Figure S3: Full redox Western blot image from Figure 2, depicting bands for Prx-3 dimer (top) and Prx-3 monomer (bottom).

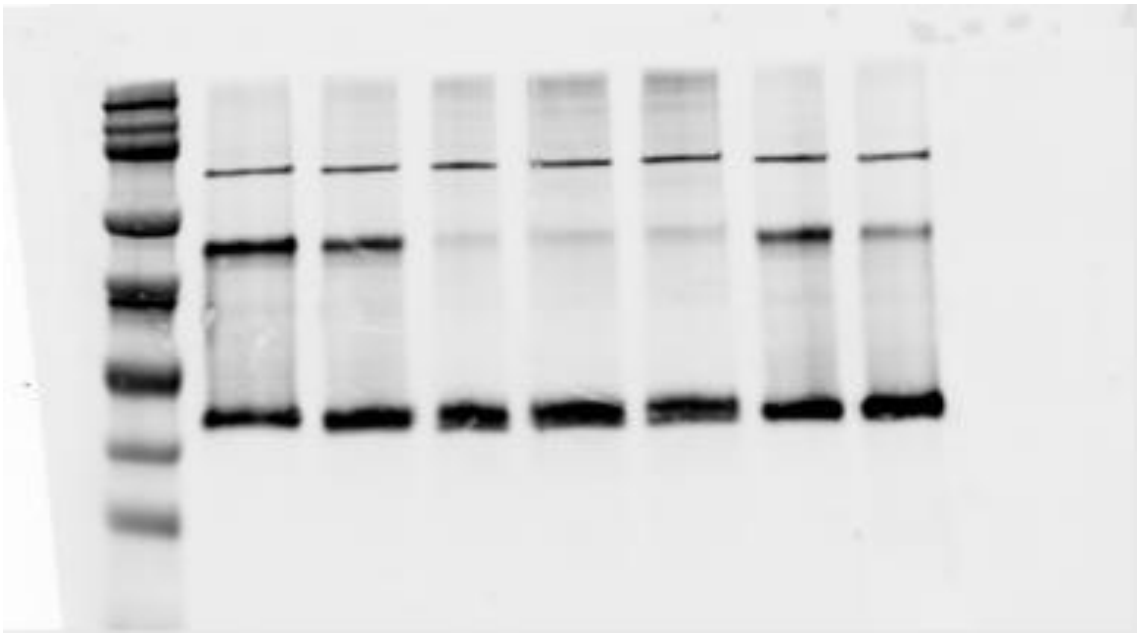

Figure S4: Full hyperoxidation Western blot image from Figure 2, depicting bands for Hsp60 (top), Prx-2 dimer (middle), and Prx-2 monomer (bottom).

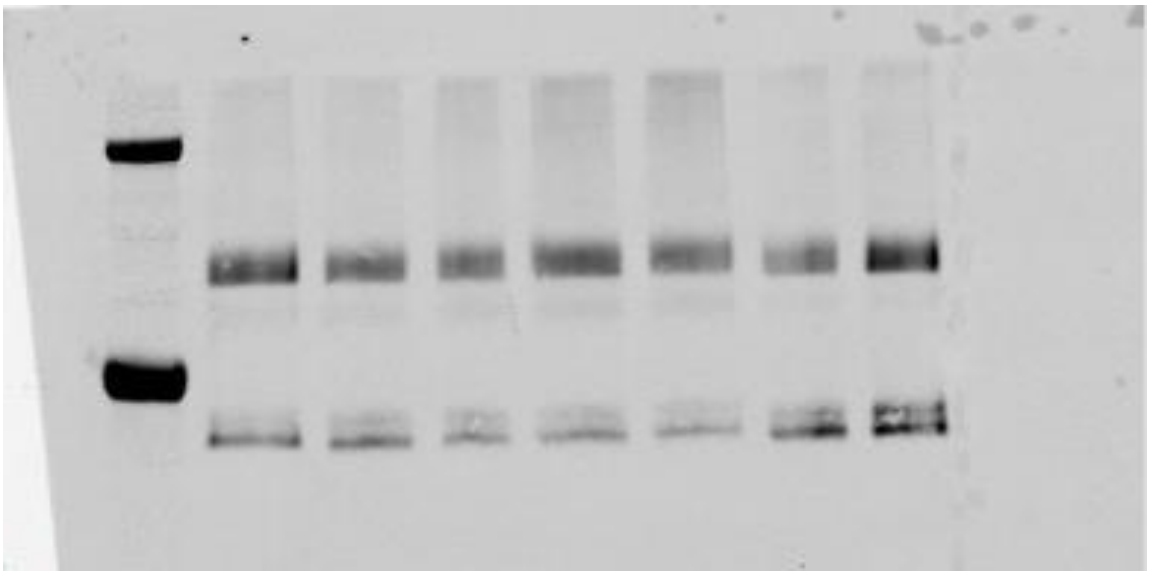

Figure S5: Full hyperoxidation Western blot image from Figure 2, depicting bands for Prx-3 dimer (top) and Prx-3 monomer (bottom).

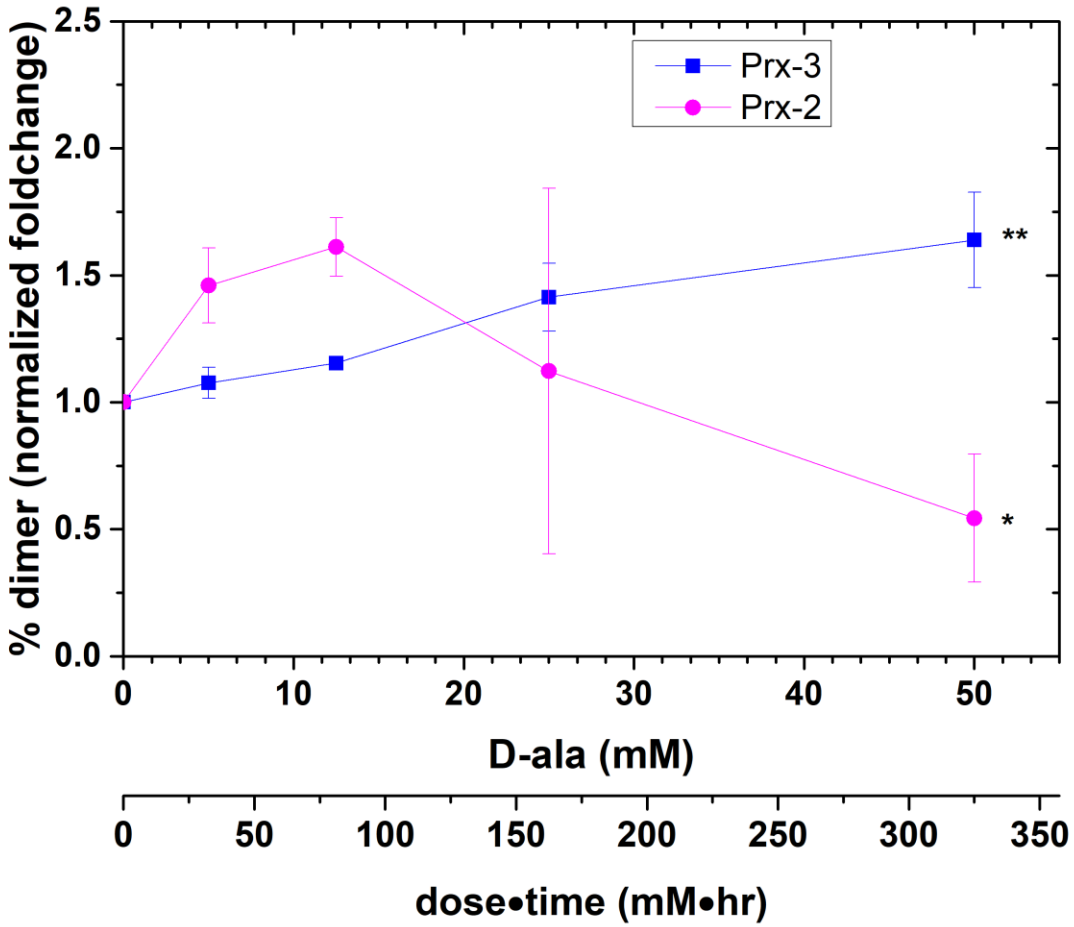

Figure S6: Densitometry plots for redox Western blot depicted in Figure 2, normalized to the intensity of the loading control Hsp60. Points represent average of two independent experiments +/- SEM. ANOVA (Prx-3) or Welch's ANOVA (Prx-2) was performed to test the trends. * indicates $P<0.1$ and ** indicates $P<0.05$ for the series.

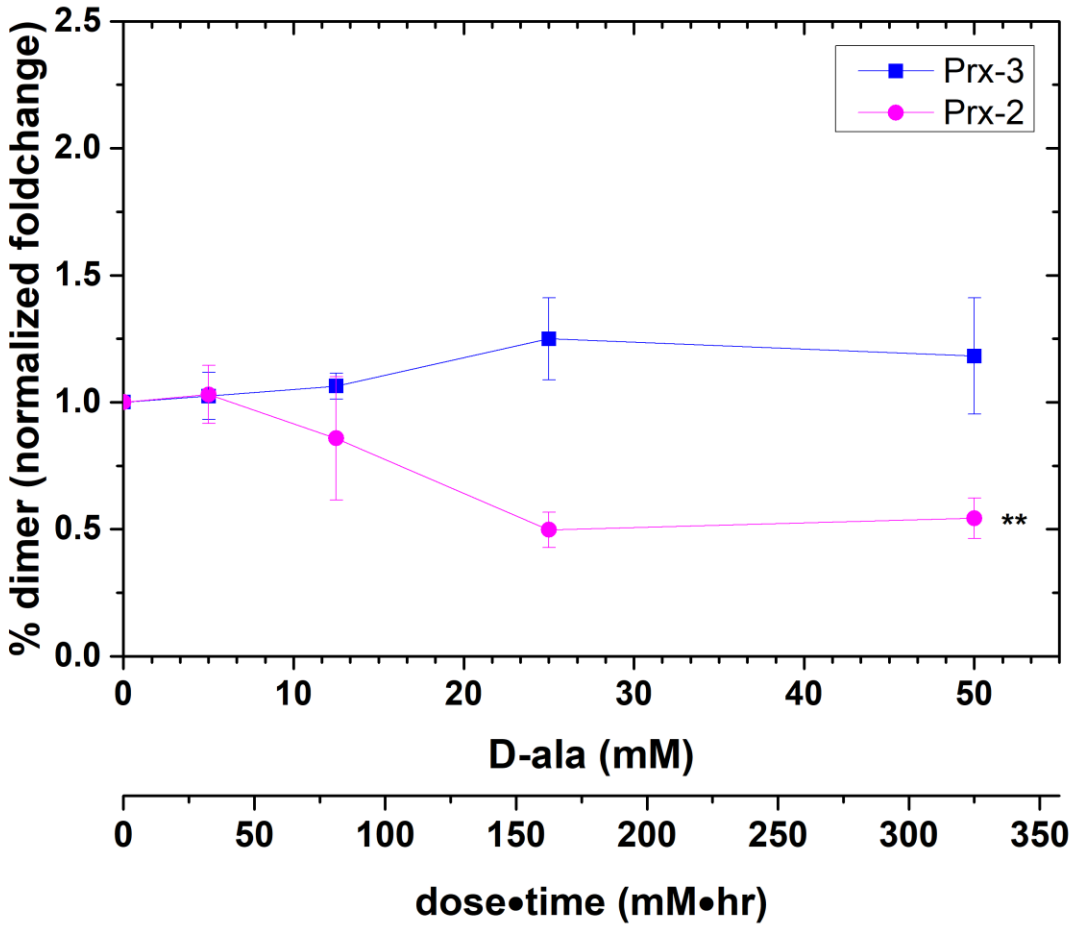

Figure S7: Densitometry plots for hyperoxidation Western blot depicted in Figure 2, normalized to the intensity of the loading control Hsp60. Points represent the average of three independent experiments +/- SEM. Welch's ANOVA was performed to test the trends. ** indicates $P<0.05$ for the series. Prx-3 data demonstrated no statistically significant trend.

Table S1: Densitometry values from Figure 2, Figure S6, and Figure S7. All numbers were normalized to the loading controls in their respective Western blots.

D-ala concentration (mM)		**Prx-3 monomer**	**Prx-3 dimer**	**Prx-2 monomer**	**Prx-2 dimer**	**Fraction Prx-3 dimer**	**Fraction Prx-2 dimer**
+MMTS	0	62156+/-24228	35131+/-22608	134912+/-9702.6	28262+/-4399.5	0.2294+/-0.0762	0.1722+/-0.0121
	5	55002+/-13592	31645+/-15355	130478+/-7435.6	45359+/-12647	0.2426+/-0.0621	0.2530+/-0.0430
	12.5	42238+/-225.62	26941+/-10338	102437+/-12125	39072+/-4695.8	0.2654+/-0.0921	0.2761+/-$3.68x10^{-3}$
	25	33727+/-4749.1	32602+/-14685	113375+/-1449.2	28015+/-18809	0.3315+/-0.151	0.1846+/-0.110
	50	28036+/-3042.1	31959+/-11227	103398+/-2741.5	10358+/-4334.0	0.3659+/-0.0641	0.09053+/-0.0368
-MMTS	0	168343+/-70401	103304+/-16894	248726+/-63181	127650+/-13120	0.4195+/-0.106	0.3598+/-0.057
	5	141375+/-38840	93877+/-11540	247723+/-55652	137910+/-33708	0.4218+/-0.101	0.3583+/-0.0231
	12.5	176510+/-69196	113229+/-7843.4	317624+/-99019	149466+/-64090	0.4432+/-0.111	0.2840+/-0.0621
	25	134234+/-47757	120969+/-20753	268272+/-68041	55391+/-14079	0.5008+/-0.0936	0.1740+/-0.0214
	50	101386+/-32385	85484+/-22418	223757+/-53016	51760+/-12977	0.4654+/-0.0867	0.1891+/-0.0221

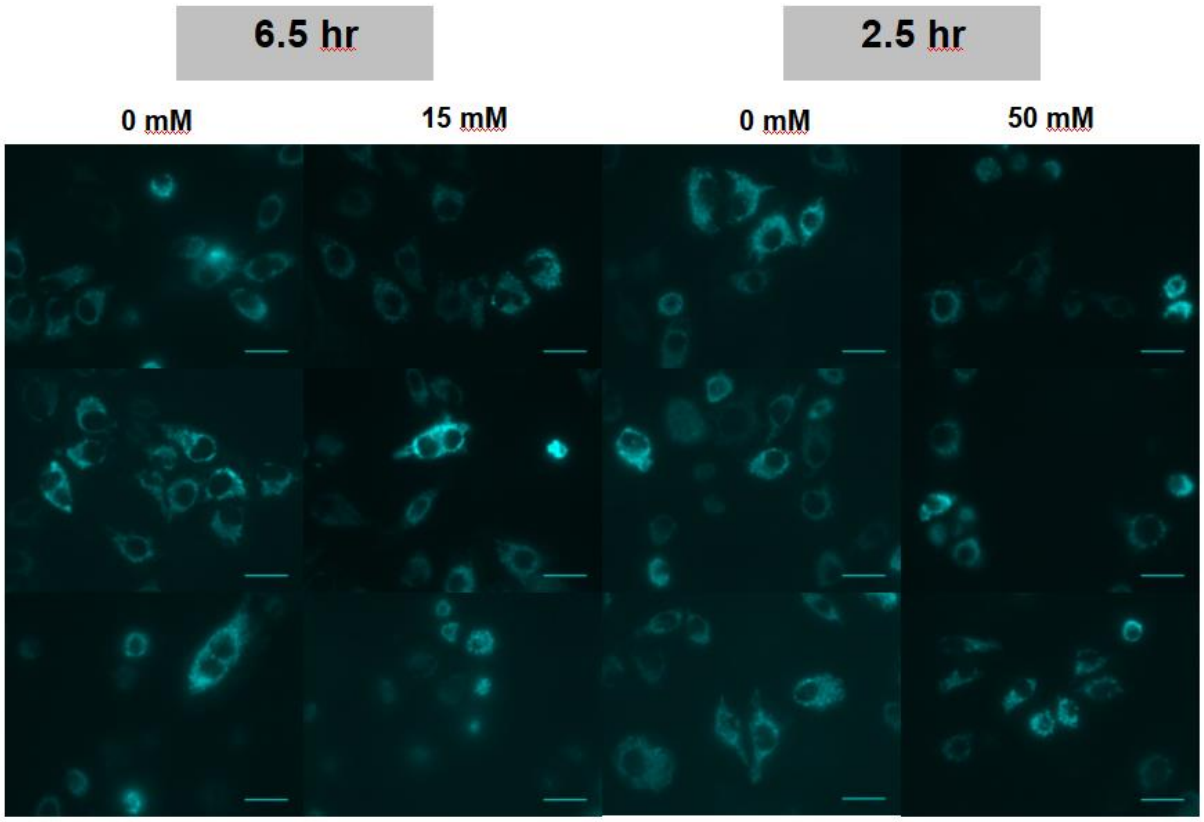

Figure S8: Supporting microscopy images for Figure 4. Scale bars represent 50 µm.

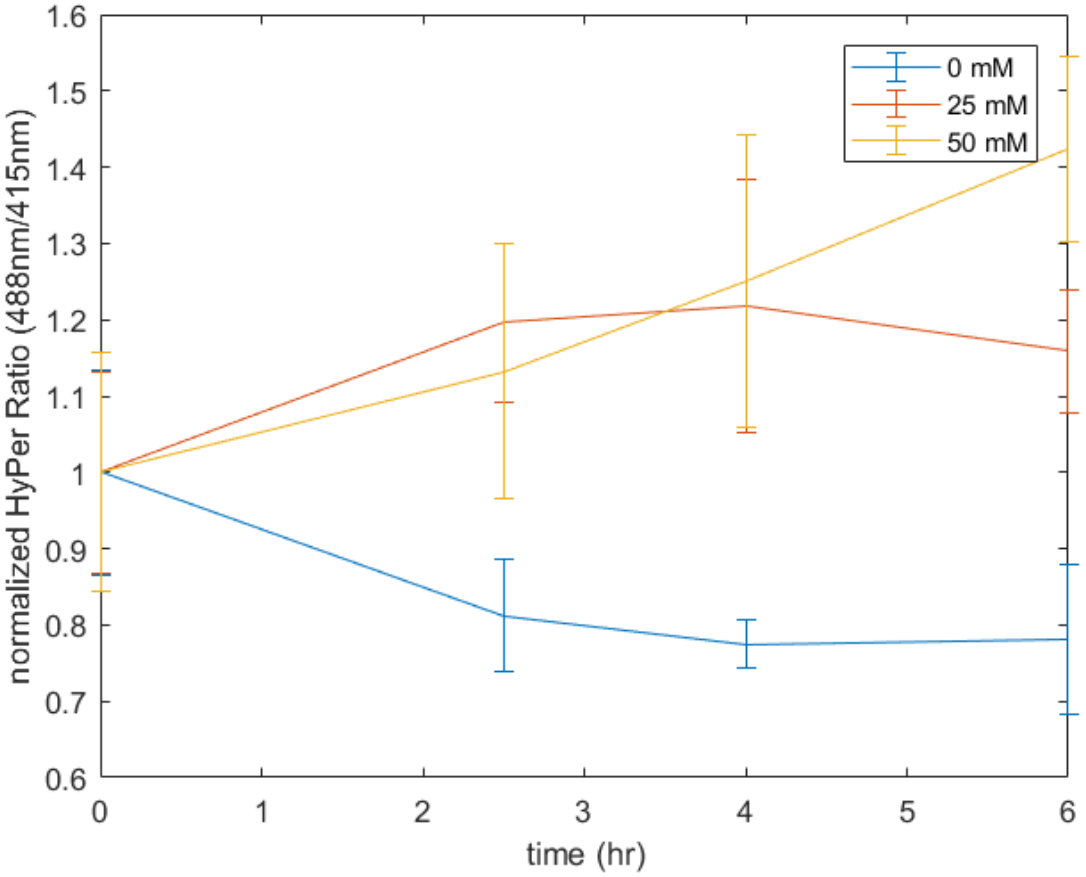

Figure S9: Normalized HyPer ratios over time for three different D-alanine concentrations. Each point represents the mean +/- std of at least 15 cells. On average, the signal from HyPer-mito increases when cells expressing DAAO are stimulated with D-ala. A large degree of cell-to-cell heterogeneity of HyPer ratios was observed, as evidenced by the error bars.

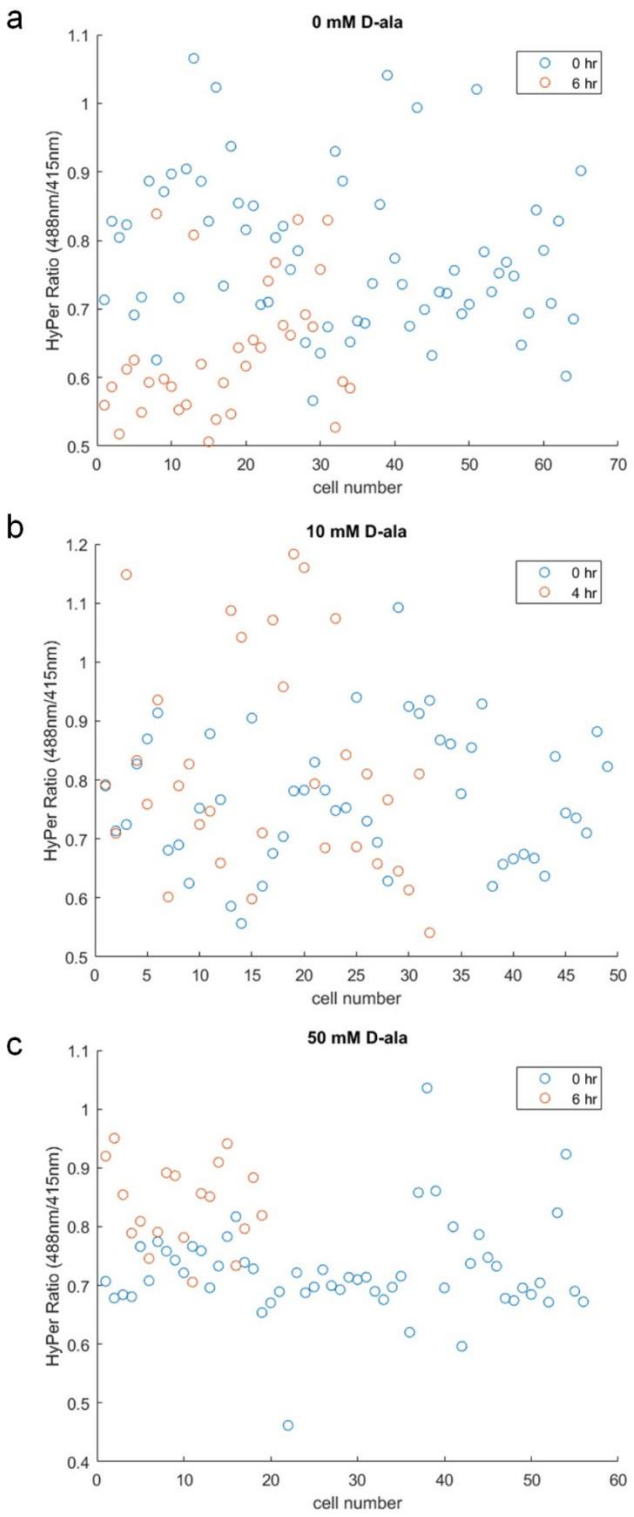

Figure S10: HyPer ratio vs. cell number for three different D-alanine concentrations, showing the significant amount of scatter in the data even without H_2O_2 perturbation (a), as well as the change in the scatter of the ratios as the cells are perturbed with H_2O_2 (b and c).

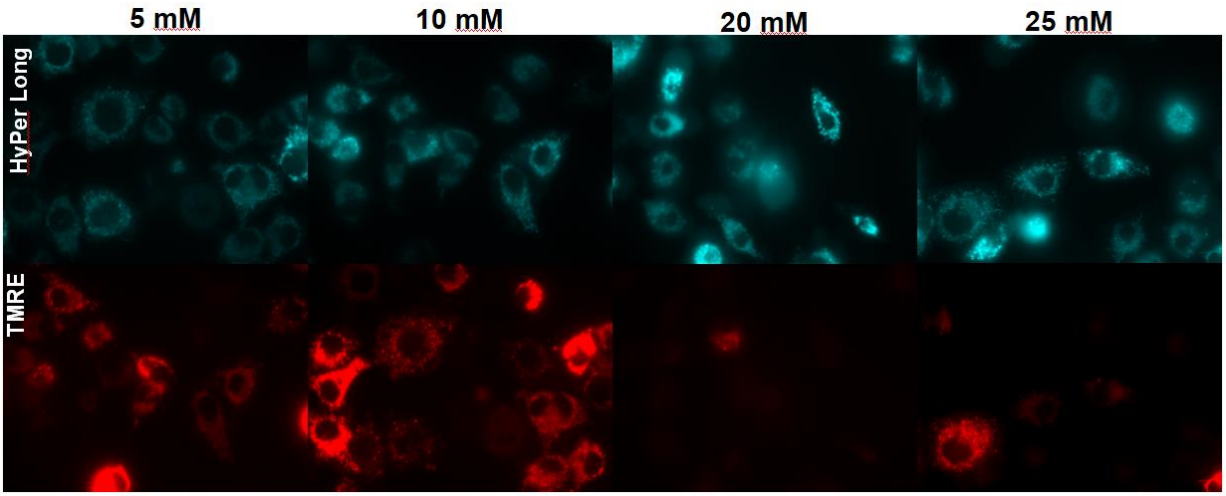

Figure S11: Microscopy plots continued from Figure 5.

***Creation of Stable Cell Lines*:**

A plasmid encoding HyPer with a mitochondrial localization tag (HyPer-mito) was purchased from Evrogen. A plasmid encoding D-amino acid oxidase with a mitochondrial localization tag (DAAO-mito) was a gift from Rajiv Ratan (Weill Medical College of Cornell University, USA). HyPer-mito and DAAO-mito were sub-cloned from their original vectors into the lentiviral transfer plasmid PLJM1-EGFP (Addgene plasmid #19319), replacing the EGFP gene between the NheI and EcoRI restriction sites. HEK293 FT cells (ATCC) were seeded at $7.5x10^5$ cells/35mm well and allowed to grow for two days until 90% confluent. The PLJM1 transfer vector containing the appropriate gene insert was co-transfected for 18 hours in OptiMEM (Invitrogen) with the packaging plasmids psPAX2 and pMD2.G (Addgene plasmids #12260 and #12259) in a ratio 3:2:1 and a total of 5 µg plasmid and 10 µg Lipofectamine 2000 (Invitrogen). Following transfection, the OptiMEM was replaced with 1 mL DMEM supplemented with 10% FBS for virus collection; viruses were harvested every 24 hours for two days. HeLa cells were seeded at a density of $3.5x10^5$ cells/35mm well and grown for 24 hours until 80-90% confluent in preparation for transfection. 1 mL virus-containing medium plus 6 µg/mL polybrene (Sigma) was added to the HeLa well for 24

hours. Cells were allowed to recover in DMEM supplemented with 10% FBS for two days, at which point they were expanded into a 10 cm dish for selection in DMEM supplemented with 10% FBS plus 6 μg/mL puromycin.

Quantification of HyPer ratios:

A rolling ball background subtraction method was applied to all images using a radius of 100 prior to quantification using ImageJ. Fluorescence intensities of individual cells were then measured in the HyPer Short (415 nm excitation) and HyPer Long (488 nm excitation). The ratio was taken as the HyPer Long intensity divided by the HyPer Short intensity. Ratios at each time point for each D-ala concentration were normalized to the average of the ratio at t=0.

Sequence for DAAO-mito construct:

Mitochondrial localization sequence (MLS) underlined

ATGTTGAGCCGCGCAGTGTGCGGCACCAGCCGGCAGCTGGCTCCGGCTTTGGGGTAT
CTGGGCTCCAGGCAGGCTAGGATGCACTCGCAGAAGCGCGTCGTTGTCCTCGGATC
AGGCGTTATCGGTCTGAGCAGCGCCCTCATCCTCGCTCGGAAGGGCTACAGCGTGCA
TATTCTCGCGCGCGACTTGCCGGAGGACGTCTCGAGCCAGACTTTCGCTTCACCATG
GGCTGGCGCGAATTGGACGCCTTTCATGACGCTTACAGACGGTCCTCGACAAGCAA
AATGGGAAGAATCGACTTTCAAGAAGTGGGTCGAGTTGGTCCCGACGGGCCATGCC
ATGTGGCTCAAGGGGACGAGGCGGTTCGCGCAGAACGAAGACGGCTTGCTCGGGCA
CTGGTACAAGGACATCACGCCAAATTACCGCCCCCTCCCATCTTCCGAATGTCCACC
TGGCGCTATCGGCGTAACCTACGACACCCTCTCCGTCCACGCACCAAAGTACTGCCA
GTACCTTGCAAGAGAGCTGCAGAAGCTCGGCGCGACGTTTGAGAGACGGACCGTTA
CGTCGCTTGAGCAGGCGTTCGACGGTGCGGATTTGGTGGTCAACGCTACGGGACTTG
GCGCCAAGTCGATTGCGGGCATCGACGACCAAGCCGCCGAGCCAATCCGCGGCCAA
ACCGTCCTCGTCAAGTCCCCATGCAAGCGATGCACGATGGACTCGTCCGACCCCGCT
TCTCCCGCCTACATCATTCCCCGACCAGGTGGCGAAGTCATCTGCGGCGGGACGTAC
GGCGTGGGAGACTGGGACTTGTCTGTCAACCCAGAGACGGTCCAGCGGATCCTCAA
GCACTGCTTGCGCCTCGACCCGACCATCTCGAGCGACGGAACGATCGAAGGCATCG
AGGTCCTCCGCCACAACGTCGGCTTGCGACCTGCACGACGAGGCGGACCCCGCGTC
GAGGCAGAACGGATCGTCCTGCCTCTCGACCGGACAAAGTCGCCCCTCTCGCTCGGC
AGGGGCAGCGCACGAGCGGCGAAGGAGAAGGAGGTCACGCTTGTGCATGCGTATG
GCTTCTCGAGTGCGGGATACCAGCAGAGTTGGGGCGCGGCGGAGGATGTCGCGCAG
CTCGTCGACGAGGCGTTCCAGCGGGACCACGGCGCGGCGCGGGAGTAG